GEANT4 Simulation of Pion Detectors for the MOLLER Experiment

A thesis submitted in partial fulfillment of the
requirement for the degree of Bachelor of Science in
Physics from the College of William and Mary in Virginia,

by

Jacob McCormick

Accepted

Advisor: Prof. David Armstrong

Prof. Gina Hoatson

Williamsburg, Virginia
May 2017

Contents

Acknowledgments

I would like to thank Professor Deconinck and Professor Armstrong for their assistance and suggestions throughout the past semester, without which the quality of my research would not be nearly as high. I would also like to express my gratitude to Kurtis Bartlett for working with me to solve various issues experienced during my research. To all other staff in the Physics Department at the College of William and Mary, I am grateful for the opportunity to perform research within such a talented group of people and for all assistance provided throughout this four year process of earning a degree.

List of Figures

List of Tables

Abstract

In an attempt to measure more precisely the parity-violating asymmetry in electron-electron (Moller) scattering, the MOLLER experiment[1] will unavoidably measure the asymmetry contribution from scattering events other than electron-electron scattering. My research focuses on electron scattering events off of the hydrogen target that produce pions. These pions have a similar energy and are bent in the same direction as the electrons, producing a contribution to the measurement of the parity-violating asymmetry. In order to measure this pion asymmetry contribution, a set of detectors will be placed downstream of a lead wall to measure a particle set that is dominated by pions. To ensure the precision of this measurement, we optimize the geometrical parameters of the detectors to maximize the light output on the Photomultiplier Tubes (PMT's). The default parameter values yield a photoelectron (PE) output from the PMT's of 259 PE's/event. From Monte Carlo simulation[2], the optimization of the light guide angle yields a ∼35% increase in PE output from 259 PE's/event to 350 PE's/event. The optimization of the light guide height yields a ∼30% increase in PE output from 340 PE's/event to 447 PE's/event. This increase in photoelectron output efficiency will help to improve the precision of our measurement of the pion background, and ultimately the precision of the parity violating asymmetry measurement in MOLLER scattering.

Chapter 1

Introduction

1.1 Background Information

The MOLLER experiment[1] is a collaborative effort between William and Mary, Jefferson Lab, and numerous other academic institutions. The experiment seeks to measure the weak interaction of the electron in Moller scattering off of a hydrogen target, as this regime yields a parity-violating asymmetry. Early theoretical evidence of parity-violating asymmetry was given by T.D. Lee, C.N. Lee, and others in the 1950's[3]. These theoretical predictions were experimentally tested in the MOLLER scattering regime by the SLAC E158 experiment, which gave an initial measurement of the asymmetry of Moller scattered electrons[4].

1.2 Motivation

The goal in this experiment is to improve upon measurements of the parity-violating asymmetry in polarized electron-electron scattering measured previously by the SLAC E158 experiment. One required step in achieving this improvement in precision is the measurement of the background from pion production. The presence of the pion background in the MOLLER experiment is discussed in detail in the theory section. The proposed pion detector uses lucite sheets, with a light guide leading to a PMT. As the pions pass through the lucite sheets, they produce Cherenkov light[5], which is directed by the light guide toward the PMT. The motivation of this research is to determine the optimum geometry for the light guides on the pion detectors using simulated data generated using the Monte Carlo simulation, GEANT 4[6]. By optimizing the geometry of the light guide and lucite detector, we can measure the pion background to a precision sufficient for the goals of the MOLLER experiment. The total parity-violating asymmetry is predicted by theory to be ~ 35 ppb, with a proposed experimental calculated precision of 0.8 ppb. The experiment expects to measure an asymmetry contribution from these pion background events of ~ 3 ppb [7]. We can use this correction to measure the parity-violating asymmetry more precisely, and compare this measurement directly to theory. If there is a statistically significant discrepancy between the two, this could be interpreted as evidence for new physics beyond the Standard Model.

Chapter 2

Theory

2.1 Parity-Violating Asymmetry

Parity in physics is an operation that reflects some vector $\vec{r}$ related to the particle to give $-\vec{r}$. In essence a parity operation perfectly inverts space. The modern Standard Model predicts a parity-violating asymmetry in polarized electron-electron scattering. The two primary interaction processes present in a Moller scattering event are the weak and electromagnetic interactions. The parity-violating asymmetry is generated by the interference term between the weak neutral current and electromagnetic amplitudes. The amplitudes of these asymmetries cannot be directly measured, so we instead measure scattering rates, which are related to the square of the sum of the two interaction mediators, η_{Z^0} and η_γ [8], given below as

$$\sigma \propto |\eta_\gamma + \eta_{Z^0}|^2 = |\eta_\gamma|^2 + \eta_{Z^0}\eta_\gamma^* + \eta_{Z^0}^*\eta_\gamma + |\eta_{Z^0}|^2 \tag{2.1}$$

where σ is the scattering rate. This equation is similar to that which describes the combination of two separate wave functions in non-relativistic quantum mechanics. Here, the term from the electromagnetic interaction, $|\eta_\gamma|^2$, is well defined by the Standard Model, and makes no asymmetry contribution. The weak interaction term, $|\eta_{Z^0}|^2$, makes a very small contribution to the total scattering rate relative to the

contribution of the electromagnetic interaction. Because of this the $|A_{Z^0}|^2$ is negligible, and our terms of interest are the interference terms[8]. The equation for the parity-violating asymmetry, A_{PV}, arising from the interference term, is given by

$$A_{PV} = \frac{\sigma_R - \sigma_L}{\sigma_R + \sigma_L} = m_e E_{Lab} \frac{G_F}{\sqrt{2}\pi\alpha} \frac{4\sin^2(\theta)}{(3+\cos^2(\theta))^2} Q_W^e \tag{2.2}$$

where m_e is the mass of the electron, E_{lab} is the energy of the electron in the lab frame, α is the fine structure constant, and G_F is the Fermi coupling constant [1]. One important point to notice is that the $\sin^2(\theta)$ term is not the weak mixing angle. This term is the center of mass angle, θ, at which the electron incident on the hydrogen target scatters. From this equation we can see that the parity-violating asymmetry is related to Q_W^e, the weak charge of the electron. Electroweak theory predicts

$$Q_W^e = 1 - 4\sin^2(\theta_W) \tag{2.3}$$

where $\sin^2(\theta_W)$ is defined as the weak mixing angle. In improving the accuracy of the measurement of the parity-violating asymmetry, we are in turn improving the accuracy of the measurement of the weak mixing angle at low energies. The weak mixing angle is a value that has been measured by multiple experiments, and is well defined by the Standard Model. If the value of the weak mixing angle is not in agreement with the value predicted by the Standard Model, then there is the possibility that there are new contributing physics processes that are not accounted for by the Standard Model. The goal of the MOLLER experiment is to search for, or constrain such new physics processes.

2.2 Pion Background

Though we are interested in electron-electron scattering, there are other interaction processes that can occur. For example, the electron from the beam can interact with a proton or neutron in the hydrogen target or its containing walls, and produce a pion as a result, through processes such as

$$e^- + p \rightarrow e^- + \Delta^+ \rightarrow e^- + n + \pi^+$$

$$e^- + p \rightarrow e^- + \Delta^+ \rightarrow e^- + p + \pi^0$$

$$e^- + n \rightarrow e^- + \Delta^0 \rightarrow e^- + p + \pi^-$$

In these interactions, the Δ^+ and Δ^0 terms are excited states of the proton and neutron, respectively. As the electron interacts with the proton, the proton is raised into an excited state. That excited proton then decays back into its stable state by production of a $\pi^{\pm}$, or π^0 [8]. This process is similar to scattering off of the neutron. In trying to isolate the asymmetry from Moller scattering events, we need a way to correct for the asymmetry that is contributed by these pion scattering events. This section will discuss some of the physical aspects of the detector, as they relate to certain essential physical processes. The physical setup will be fully discussed in the experimental setup section. These physical processes include Cherenkov radiation, electromagnetic showering, and total internal reflection.

2.3 Cherenkov Radiation

We use the Cherenkov process as the means to produce optical photons as pions pass through the lucite detector. As a particle passes through the lucite, the local speed of light changes. As charged particles pass from the open air to the lucite medium, their velocities may be greater than the speed of light in lucite. As a result these particles radiate, producing Cherenkov light. This Cherenkov light provides a means to turn this detection event into a measurable signal in the PMT [9].

2.4 Electromagnetic Showering

The majority of scattered particles are electrons, and we are trying to isolate the small pion background to these desired electron events. We use the process of electromagnetic showering to isolate pions for detection by the PMT's. This is accomplished using a thickness between 25 and 50 cm of lead absorber after the main detector and before the pion detector apparatus. As the particles pass through the high Z lead wall, the electrons are more likely to be disturbed by the lead atoms. This disturbance creates a probability of the particles losing energy through the process of electromagnetic showering. The pions are less likely to lose energy by this process because they are an order of magnitude more massive than the electrons; 0.5 MeV vs. roughly 140 MeV. This large mass difference between the two particles makes the pions less likely to radiate as a result of deceleration via interaction with the lead nuclei. As a result, most of the incident electrons will be stopped in the lead, dramatically reducing the ratio of electrons to pions behind the lead wall. This helps to ensure that the parity violating asymmetry measurement at the pion detectors is primarily due to pion events, allowing for a corrective measurement to be applied to the main detector measurement.

2.5 Total Internal Reflection

In order to guide the Cherenkov light to the PMT's, we use a combination of total internal reflection and reflection using reflective mylar sheets. The majority of photons will reflect internally in the lucite volume. However, if the angle of impact of the photons on the lucite surface is sufficiently steep, then an outer layer of mylar sheet reflects the photons back into the lucite volume. These two methods of reflection help to ensure that the photons only have the option to escape the lucite volume into the light guide, to be guided to the PMT face.

Chapter 3

Experimental Setup

3.1 Full MOLLER Experiment

The experiment will use the 11 GeV electron beam at Jefferson Lab to provide longitudinally-polarized electrons for scattering off of the liquid hydrogen target. The scattered particle trajectories will then be bent by a toroidal magnet depending on the energy of the scattered particle. The particles will pass through collimators to select scattered particles with energies consistent with the Moller scattering regime. The selected particles will then reach the main detector. The main detector consists of quartz Cherenkov radiators that are read out by PMT's. The main detector will use a geometry similar to that of the pion detector array, with light guides used to direct the light toward the PMT face. A visual model of the planned apparatus is provided in figure 3.1.

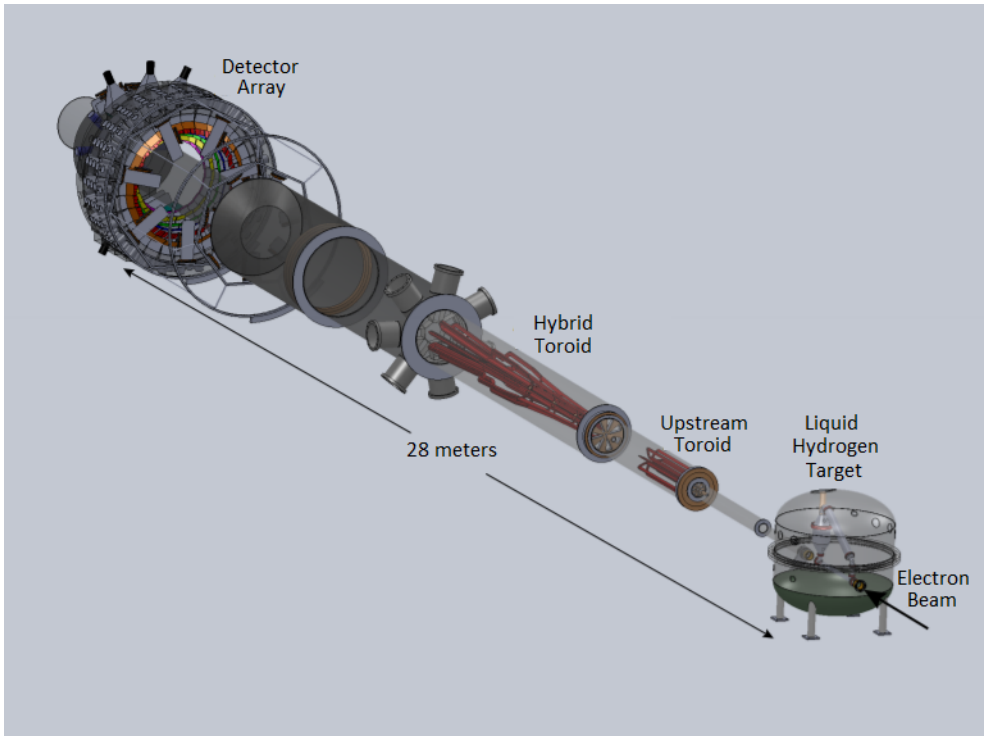

Figure 3.1: Visual model of the MOLLER experiment. [10]

3.2 Pion Detector Array

After passing through the main detector array, the scattered particles will then pass through a lead wall. The majority of particles that successfully pass through the lead wall will be pions because, as described earlier, the electrons shower electromagnetically in the lead, depositing most of their energy into the lead. After the lead wall is a detector array for detecting the pion background. The detector array has layered lucite, coincident trigger scintillators, and a calorimeter at the back. The trigger scintillators will serve as a fast time reference for tracking particles that have passed through the lead wall, and the calorimeter will be used to measure the energy of the incident pions[8]. Coupled to the layered lucite sheets will be a light guide that directs light from the lucite to the PMT. A visualization of this setup is given in figure 3.2. Here X_0 is the radiation length of the electrons through the lead absorber.

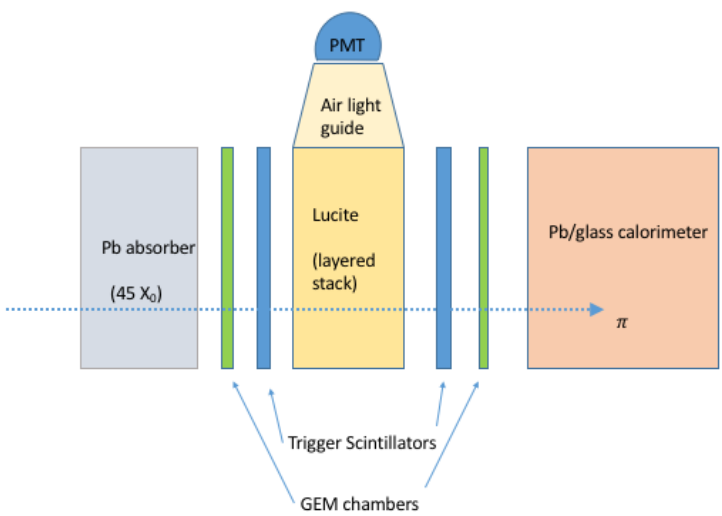

Figure 3.2: Visual Model of the pion detector. [11]

The interest of this research is focused on the lucite block and air light guide. Varying parameters associated with these two geometrical objects will affect the amount of light that hits the PMT's. The goal is to find the geometrical parameter values that maximize light output on the PMT face. This ensures that we get a strong, clear signal for the measurement of the pion background.

Chapter 4

Current Progress

4.1 Optimization of Light Guide Angle

Much like the previous semester, the beginning of the semester was spent becoming familiar with using C scripts to analyze ROOT[12] files produced by the Geant4 simulation. The geometry of the pion detector is changed using the associated Geometry Description Markup Language (GDML)[13] files. Much of the geometry was specified using common variables, allowing for each of the geometrical parameters to be changed with relative ease. The six original parameters of interest were light guide angle, light guide height, lucite angle, lucite height, lucite outside width, and lucite inside width. These parameters are illustrated in figure 4.1.

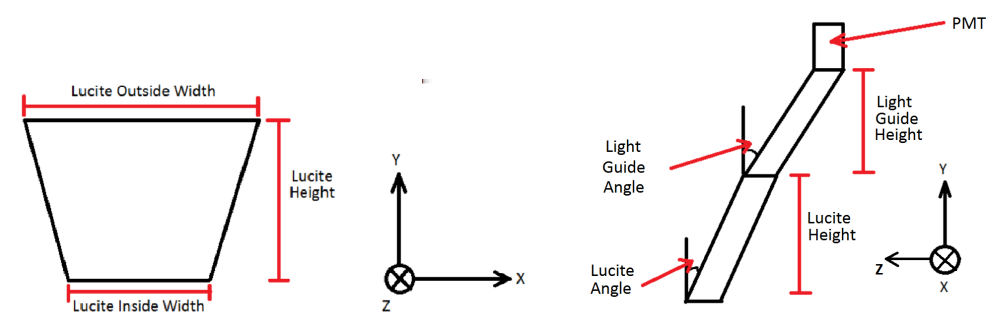

Figure 4.1: Representation of the geometrical parameters of the light guide and lucite. The z axis is aligned with the direction of the beam of electrons incident on the hydrogen target.

The optimizing procedure for this research is given below. First, each of the parameters is preloaded with a value. Then, one parameter is varied until an optimal value was found. An optimal value occurs when the number of photons incident on the face of the PMT's is maximized. Once that optimal value is found, it is saved and another parameter value is varied. This process continues until a globally optimal parameter array is produced which yields the highest number of photons contacting the PMT face.

The first parameter to be varied is the light guide angle. The simulation is run for a large range of light guide angle values. These values, and the resulting data for these light guide angle values, are provided in table 4.1. We are interested in measuring the mean number of photelectrons detected on the PMT face. This value takes into account the efficiency of the PMT in converting photons incident on the PMT face to photoelectrons. These photoelectrons produce a current which can be measured by the PMT. The default light angle is -45°.

Light Guide Angle (degrees)	Mean Number of Photoelectrons at PMT	Error of Mean	Std. Dev.	Error of Std. Dev.
-45	259.3	11.5	143	8.1
-40	317.5	12.8	162	9.1
-35	315.1	13.5	181.5	9.6
-30	330	11.7	150.4	8.3
-25	334.5	12.1	156.2	8.5
-22.5	350.5	11.4	165.3	8.1
-20	351.6	10.8	144.5	7.6
-10	347.7	12.9	159.6	9.2
0	349.1	14.6	177.7	10.3
10	335.2	14.7	191.8	10.4
20	336.8	13.4	179.3	9.5
30	305.9	11	143.1	7.8

Table 4.1: Table of values associated with optimization of light guide angle.

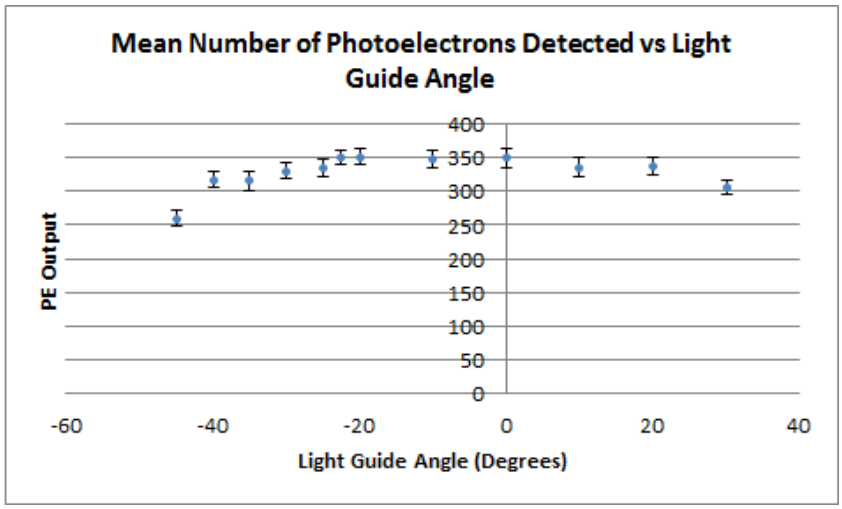

Figure 4.2: Graph of mean number of photoelectrons versus light guide angle.

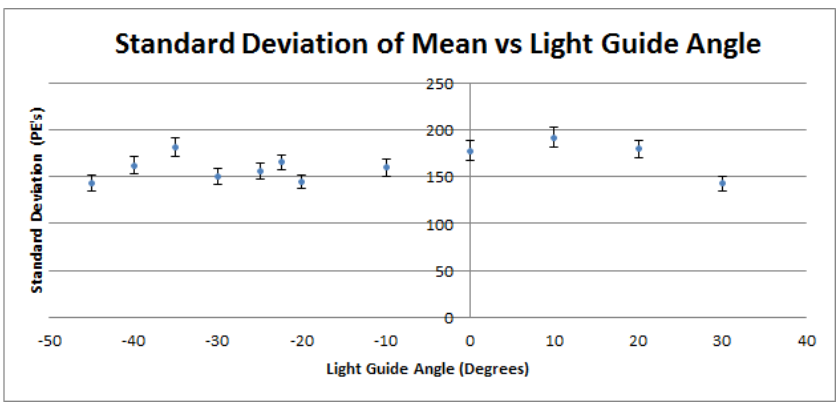

Figure 4.3: Graph of standard deviation of the mean versus light guide angle.

The value -22.5° is chosen as the optimal value for the light guide angle due to a misconception regarding the detector geometery. This light guide angle was chosen with the idea that part of the Cherenkov cone produced within the lucite would track parallel to the light guide. In order to be parallel with the Cherenkov cone, $\theta_c - 90°$ must be chosen for the light guide angle, where θ_c is the Cherenkov angle. Photoelectron output increases from 259 PE's/event to 350 PE's/event, or a ∼35% increase, however there is further optimization necessary for this parameter.

4.2 Optimization of Light Guide Height

Following the optimization of the light guide angle, the next parameter value to be varied is the light guide height. The table of light guide height values, as well as the results of simulation, are given table 4.2. The default value for the light guide height is given as 25 centimeters.

Light Guide Height (cm)	Mean Number of Photoelectrons at PMT	Error of Mean	Std. Dev.	Error of Std. Dev.
5	446.9	14.1	177.9	10
10	419.6	13.6	187.5	9.6
15	351.7	13.8	177.8	9.8
20	348.1	12.8	168.8	9.1
25	340.9	11.9	154.2	8.4
30	306.0	10.1	124.9	7.2
35	304.7	13.3	175.5	9.4
40	284.8	11.2	144.2	7.9
45	272.9	10.5	139.0	7.4
50	240.0	11.3	151.4	8.0

Table 4.2: Table of values associated with optimization of light guide height.

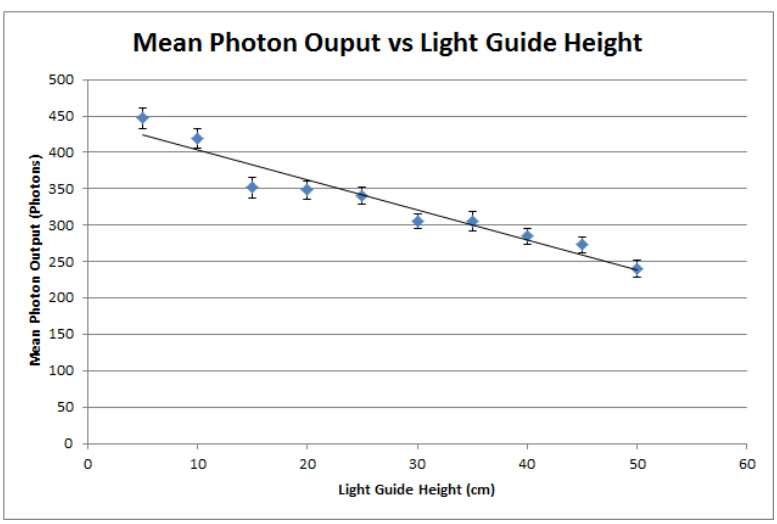

Figure 4.4: Graph of mean number of photoelectrons versus light guide height.

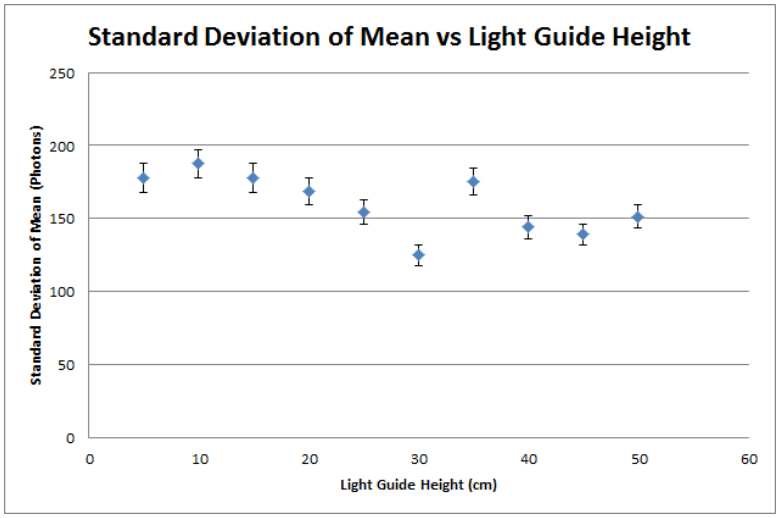

Figure 4.5: Graph of standard deviation of the mean versus light guide height.

The graph of the mean photoelectron output suggests that the optimal value occurs at or near 0 cm. This optimization yields an increase in photoelectron output from 340 PE's/event to 447 PE's/event, or a ∼30% increase in photoelectron production for each event. The simulation data implies that it would be more efficient for us not to use a light guide for the pion detector array at all. This seems counter-intuitive, as the implementation of light guides in detector design is relatively standard. One explanation for the result is the possibility is that the light guide actually reflects many of the photons back into the lucite. A depiction of two possible photons reflection processes that may be occurring is given in figure 4.6. The geometry is exaggerated to help emphasize the reflection process occurring and its potential implications.

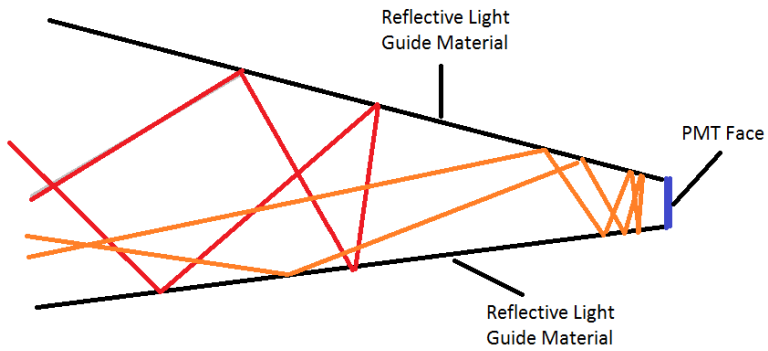

Figure 4.6: We can see that with a more aggressive reflection angle, the photon is quickly reflected back. Even with a more shallow reflection angle, there is still a chance that the photon is reflected back into the lucite.

4.3 Optimization of PMT Diameter

Next, the cost of the PMT's is taken into account, and we attempt to find a PMT configuration that maximizes output while minimizing cost. This is ongoing, however preliminary results of variation of the diameter of the PMT face are given in table 4.3. It is important to note that larger diameter PMT's are significantly more expensive that those with smaller diameters.

PMT diameter (in)	Mean Number of Photoelectrons/in^2	Error of Mean/in^2	Std. Dev.	Error of Std. Dev.
1.5	26.0	1.8	42.8	2.3
2.0	27.8	2.1	88.0	4.6
2.5	24.3	1.3	82.1	4.4
3.0	23.3	1.1	100.5	5.4
3.5	23.0	1.1	145.6	7.5
4.0	21.4	0.9	152.8	8.2
4.5	21.1	0.8	169.0	9.0
5.0	19.7	0.7	167.4	9.1

Table 4.3: Table of values associated with optimization of PMT diameter.

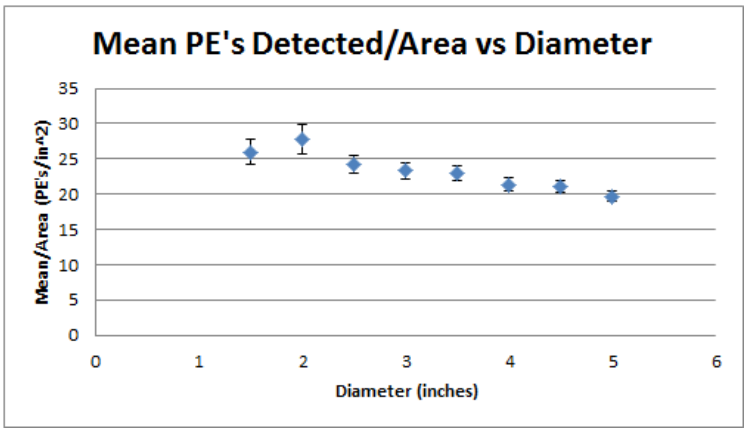

Figure 4.7: Graph of mean number of PE's per unit area versus PMT diameter.

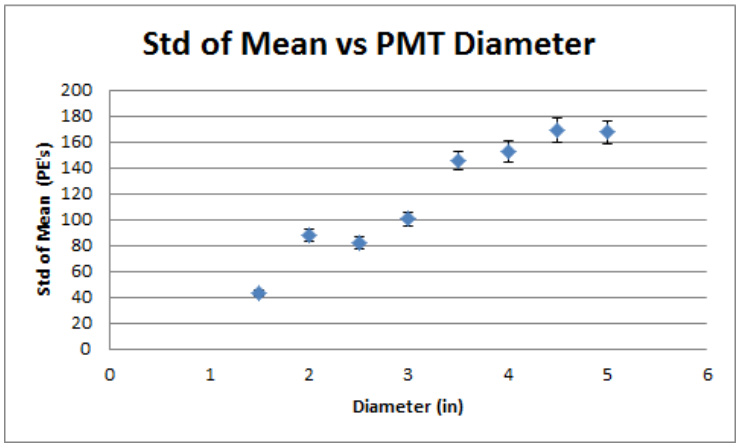

Figure 4.8: Graph of standard deviation of the mean versus PMT diameter.

The graph of the mean output efficiency (how many photoelectrons are produced for every square inch of area on the PMT face) vs. diameter suggests that the most area efficient PMT diameter is 2 in. For this section, we are not as interested in which diameter value maximizes photoelectron output. Instead we are interested in maintain adequate photelectron production (100-200 PE's/event) while minimizing the cost of the PMT. The most area efficiency PMT diameter, 2 in, only produces about 87 PE's/event, which is well below the adequate photoelectron production threshold. As a result, more research must be performed to find an optimal value.

Chapter 5

Future Research

It is necessary to optimize the light guide angle along with the lucite angle. Scanning over a larger range of negative angles may yield a new global maximum photoelectron output. This second optimization will account for the incorrect interpretation of the detector geometry. The next step is the optimization of the other geometrical parameters associated with the pion detectors. This will help to determine the globally optimal detector geometry to most effectively channel Cherenkov light from the lucite sheets into the PMT's. Another consideration to be tested is the implementation of PMT's with smaller sensitive faces. PMT's with smaller diameters cost significantly less than the 5 inch diameter PMT's that are currently being considered for use. We must also consider the physical consequences of not using a light guide for the PMT's. Having the PMT's closer to the scattered beam increases the chance of false hits occurring. A false signal can be produced if the pions, or other particles, pass directly through the PMT instead of the lucite. Therefore, as we move forward in this research, it is important to continue to consider the balance between cost-savings and efficiency.

Chapter 6

Citations

[1] The MOLLER Collaboration, 2014 Dec 3. *The MOLLER Experiment: An Ultra-Precise Measurement of the Weak Mixing Angle using Mller Scattering.* https://arxiv.org/pdf/1411.4088v2.pdf

[2] Angelis, Alessandro, 2001 Sep. *The GEANT 4 Toolkit.* http://www.fisica.uniud.it/ deangeli/test/g4aquila01.pdf

[3] Lee, T. D., C. N. Yang, 1986. *Question of Parity Conservation in Weak Interactions.* http://www.physics.utah.edu/ belz/phys5110/PhysRev.104.254.pdf.

[4] SLAC E158 Collaboration, 2005 Aug 19. *Precision Measurement of the Weak Mixing Angle in Mller Scattering.* http://journals.aps.org/prl/pdf/10.1103/PhysRevLett.95.081601

[5] Particle Data Group, 2014 Aug 21. *Passage of Particles Through Matter, 32.7.* http://pdg.lbl.gov/2014/reviews/rpp2014-rev-passage-particles-matter.pdf

[6] http://geant4.cern.ch/

[7] The MOLLER Collaboration, 2016 Dec 9. *The MOLLER Experiment: An Ultra-Precise Measurement of the Weak Mixing Angle Using Moller Scattering.* http://physics.wm.edu/ armd/MOLLER_dircd1.pdf

[8] Conversations with David Armstrong.

[9] The Particle Data Group, 2016 *2016 Review of Particle Physics.* http://pdg.lbl.gov/2016/download/rpp-2016-booklet.pdf

[10] The MOLLER Collaboration, 2011 Sept 12. *The MOLLER Experiment: An Ultra-Precise Measurement of the Weak Mixing Angle Using Moller Scattering.* http://people.umass.edu/kkumar/images/DOE_Moller.pdf

[11] Armstrong, David, 2016 Nov 2. *Current MOLLER pion detector concept.* Dilbert Elog. https://dilbert.physics.wm.edu/MOLLER+Simulation/72

[12] https://root.cern.ch/root/html/tutorials/

[13] https://gdml.web.cern.ch/GDML/